J. Adhesion Sci. Technol., Vol. 17, No. 10, pp. 1385–1401 (2003)

Also available online - www.vsppub.com

The effect of liquid-induced adhesion changes on the interfacial shear strength between self-assembled monolayers

DMITRI V. VEZENOV [1,*], ALEKSANDR NOY [1,†]
and CHARLES M. LIEBER [1,2]

[1] *Department of Chemistry and Chemical Biology, Harvard University, Cambridge, MA 02138, USA*
[2] *Division of Applied Sciences and Engineering, Harvard University, Cambridge, MA 02138, USA*

Received in final form 7 May 2003

Abstract—Friction between chemically-modified tips and surfaces has been studied with chemical force microscopy (CFM) to evaluate the effect of changing solid/liquid free energy on energy dissipation in sliding tip–surface contact. Well-controlled conditions were necessary to attain a single asperity contact in these experiments. We found that in a series of methanol–water mixtures the interfacial shear strength between CH_3-terminated surfaces of the siloxane self-assembled monolayers (SAMs) was independent of the adhesion force. The shear strength value of 10.2 ± 1.0 MPa found for this interface under methanol–water media is consistent with the previous studies of similar systems under dry gas conditions. A comparison to available data on interfacial shear strengths demonstrated that siloxane monolayers were much more effective in reducing friction than various carbon coatings.

Keywords: Interfacial shear strength; chemical force microscopy; self-assembled monolayers; friction; adhesion; contact mechanics; surface free energy.

1. INTRODUCTION

Friction at a molecular level has been studied in considerable detail in recent years [1–7] owing to significant improvements in instrumentation, force probe calibration and characterization [8–11], and control of the chemical terminal functionality [12] at the sheared interface. The relationships between frictional energy dissipation,

*To whom correspondence should be addressed at: NANOPTEK Corporation, P.O. Box 1542, Concord, MA 01742, USA. Phone: (978)-371-7339. Fax: (978)-369-7733.
E-mail: dvezenov@nanoptek.com

†Present address: L-234, Chemistry and Materials Science Directorate, Lawrence Livermore National Laboratory, Livermore, CA 94550, USA.

interfacial intermolecular interactions and applied load have been studied most successfully with point contact experiments using scanning or interfacial force microscopes. In developing fundamental understanding of these relationships, an important role was played by the model systems based on the self-assembled monolayers (SAMs) chemically anchored to a supporting substrate. The friction performance of the SAM system is also of significant technological interest for reducing friction in the silicon based microelectromechanical devices [13, 14].

Because of the importance of mapping surface interactions in a variety of problems, the concept of chemical force microscopy (CFM) has been introduced [15] that exploits specifically functionalized force probes to study intermolecular interactions on a nanometer scale. This approach provides a reproducible way to control the chemical identity and surface energy of the probe by covalently linking a self-assembled monolayer terminating in a distinct functional group to the tip surface. Chemical modification of the scanning probe microscope (SPM) tips eliminates uncertainties in terminal functionality associated with using unmodified and often contaminated microfabricated tips and allows one to study interactions between chosen distinct pairs of organic functional groups. The flexibility in varying the tip chemistry combined with the sensitivity and resolving power of the SPM yields a technique capable of studying intermolecular interactions on a nanometer scale [12] and, specifically, allows one to characterize the effect of the surface chemistry on the interfacial shear strength.

Under ambient conditions, it is difficult to distinguish true chemical contributions to friction from other factors, mostly because a large magnitude of the capillary adhesion can produce normal loads drastically higher than the externally applied loads or contributions of the surface forces [16]. Due to the capillary condensation in air of finite relative humidity, SPM measurements of the interfacial strength between the same tip and thin film (amorphous carbon or diamond) sample pairs showed an increase by a factor of 2–3 as compared to the dry inert atmosphere, although the reasons for the increase were not clearly understood [5]. This capillary effect can be eliminated by performing measurements in either liquids or ultrahigh vacuum. Force measurements between organic functional groups have been typically performed under liquid media [12], whereas ultrahigh vacuum or dry inert atmosphere studies focused predominantly on clean silicon or metallic probes and inorganic substrates [2–5, 17].

Friction forces between tips and samples modified with different functional groups have been measured in ethanol [18], water and dry argon [19] as a function of the external load. In these measurements, the friction forces were found to increase linearly with the applied load. At a fixed loading, the absolute friction force decreased as $COOH/COOH > CH_3/CH_3 > COOH/CH_3$ [18, 19]. The trend in the magnitude of the friction forces and friction coefficients was the same as that observed for the adhesion forces: COOH/COOH-terminated tips and samples yielded large friction and adhesion forces, while the $COOH/CH_3$ combination displayed the lowest friction and adhesion. Similarly, in aqueous

solutions [20] the adhesion and friction forces followed the parallel trends for hydrophilic functional group pairs: COOH/COOH > COOH/OH > OH/OH > COO^-/OH > COO^-/COO^-. Thus, there appeared to be a direct correlation between the friction and adhesion forces measured between well-defined SAM surfaces. Surface force apparatus (SFA) studies of structurally similar layers also show that the friction force correlates with the force of adhesion [21]. In contrast, a better correlation with adhesion hysteresis and not the adhesion force was found in SFA studies of dissimilar phases (i.e. crystalline, amorphous and liquid-like) of different hydrocarbon surfactants [22–25]. For similar functional groups, the friction was also found to be strongly affected by the structural characteristics of the monolayer, and dependence of friction forces on the chain length has been reported [26]. Recently, we have demonstrated [27] that solvation energy is an important factor in determining adhesion between organic groups in liquids and can change by more than an order of magnitude even for the same tip–sample pair if the strength of liquid–liquid interactions is varied.

In this paper, we investigated the effect of the medium on friction forces between chemically modified tips and samples. We found that the interfacial shear strength for CH_3-terminated surfaces was independent of the overall adhesion force (surface free energy) when adhesion level changed due to the variations in the liquid medium. This behavior clearly indicates that the liquid is excluded from the tip–sample contact zone in the AFM experiments. We also clarify the origin of the correlation between adhesion and friction forces: higher adhesion forces lead to increase in tip–sample contact area and thus to higher friction force.

2. EXPERIMENTAL SECTION

2.1. Sample and tip preparation

Preparation of substrates and AFM probes for chemical modification with SAMs involves either (1) coating the surfaces of the tips or Si substrates with a layer of gold for modification with thiol SAMs, or (2) oxidative cleaning of the Si substrates and silicon nitride tips for subsequent modification with silanes. Au coating was accomplished using conventional e-beam deposition technique: substrates (Si(100) wafers, Silicon Sense, Nashua, NH, USA; test grade, 500 μm thick) and commercial silicon nitride tip-cantilever assemblies (Digital Instruments, Santa Barbara, CA, USA) were coated (base pressure 10^{-7} torr) with a 5-nm adhesion layer of Cr followed by 100 nm of Au at the rate of 0.1 nm/s. For deposition at room temperature, the typical grain size of the resulting Au(111) surface was between 50 and 150 nm.

Hexadecanethiol (Aldrich, Milwaukee, WI, USA) and octadecyltrichlorosilane (OTS, Aldrich) were purified by vacuum distillation. Thiolate monolayers were formed by immersion of the freshly Au-coated substrates and Au- or Ag-coated probe tips in 2–3 mM ethanol solution of thiol for at least 2 h immediately

after metal deposition. Methyl-terminated siloxane monolayers were prepared by immersing freshly cleaned (piranha solution, 1 : 2 mixture of H_2O_2 and H_2SO_4, 90°C, 20 min) Si(100) substrates and Si_3N_4 tip-cantilever assemblies pretreated in oxygen plasma (10 min) in a 20 mM toluene solution of OTS for 3 h. Before use or characterization, all SAM substrates were rinsed in EtOH and dried with a stream of dry N_2.

2.2. *Friction measurements*

Adhesion and friction-force measurements in liquid media were made with a Nanoscope III Multi-Mode scanning force microscope (Digital Instruments) equipped with a fluid cell. With the scanning force microscope, the adhesion interaction between different functional groups is determined from force *versus* sample displacement (F–D) curves. In these measurements, the deflection of the cantilever is recorded during the sample approach–withdrawal cycle. The observed cantilever deflection is converted into a force using the cantilever spring constant. The pull-off force determined from the jump in the retracting part of the cycle corresponds to the adhesion between functional groups on the tip and sample surface.

The lateral (friction) force was measured by recording traces of cantilever lateral deflection ('friction loops') while the sample was rastered back and forth using the piezoscanner. Friction force values were determined from lateral force traces, each containing 512 data points, by averaging the differences in friction forces observed when scanning over a 10-μm distance in opposite directions at 80 μm/s. The resulting lateral deflection traces were converted into forces using the lateral spring constant for the AFM tip. The externally applied load was controlled independently through the cantilever normal deflection. Friction *versus* load (F–L) curves were obtained from the data for Au-coated tips and samples. The same procedure was used previously [18, 20] in determining friction forces in terms of friction coefficients for several combinations of the tip–sample functional groups.

Frictional forces as a function of applied load between modified tips and samples were also measured using a lock-in detection scheme [28]. Briefly, the sample is scanned slowly in a vertical (z) direction (approx. 5–10 s per approach–withdrawal cycle, $\Delta z = 100$–300 nm) and at the same time rastered laterally in the direction perpendicular to the cantilever symmetry axis (y) at a much higher frequency (3–5 kHz, $\Delta y = 10$–30 nm, i.e. at a tip velocity of 60–300 μm/s), but away from the piezotube resonance frequency (determined to be approx. 10 kHz, J scanner). The vertical deflection signal is then recorded as usual, while the lateral signal is fed into a lock-in amplifier (model 124A, EG&G Princeton Applied Research Corporation, Princeton, NJ, USA). The output of the lock-in amplifier is then recorded by the Nanoscope software from auxiliary channel of the AFM controller as the friction signal simultaneously with the cantilever's normal deflection.

2.3. Force calibration

Normal sensitivity of the detector was determined from the linear compliance region of F–D curves. For a Digital Instruments Nanoscope III scanning force microscope equipped with a fluid cell, the normal sensitivity (in the liquid) was typically around 0.01 and 0.02 V/nm of z axis piezotube displacement for 220 μm and 110 μm long cantilevers, respectively.

Lateral sensitivity was determined from the static friction portion of the atomic stick–slip friction loops on mica and typically was 0.25–0.35 V/nm of x axis piezotube displacement [29]. However, recent work [7, 30] demonstrated that lateral sensitivities determined in this way were underestimated for soft substrates such as mica, because contact stiffness and even tip apex stiffness of high aspect ratio tips were comparable to the lateral stiffness of the cantilever. This becomes apparent when the lateral sensitivity is determined from stick–slip friction loops taken at different normal loads. The higher external force results in a larger contact area and, hence, the stiffness of the contact increases (Fig. 1). This brings apparent lateral sensitivity closer to its true value. There are several ways to deal with this problem: (1) record friction loops on sloped surfaces with known slope angles (two different slopes on the same substrate are required); (2) use longitudinal stiffness of the cantilever to perform friction measurements — in this case normal sensitivity is used in calculations of friction forces; (3) relate lateral sensitivity to normal sensitivity; or (4) fit the lateral detector response at different external forces to available contact mechanics models. We used sensitivity values determined from the atomic stick–slip friction loops and applied the aforementioned methods 3 and 4 to arrive at the actual values of the lateral sensitivity.

Cantilever spring constants were found by the thermal resonance method developed by Hutter and Bechhoefer [10]. Normal spring constant for Au-coated standard 220-μm-long Si_3N_4 cantilevers (Nanoprobes, Digital Instruments) determined from the power spectral density spectrum of the thermally excited cantilever motion was 0.11 ± 0.01 N/m. Lateral spring constants were calculated based on the relationship between normal and lateral constants. Normal spring constants for OTS modified 110-μm-long Si_3N_4 cantilevers were 0.2 N/m, with a $k_{\text{lateral}}/k_{\text{normal}}$ ratio of 502, calculated according to Hazel and Tsukruk [31].

2.4. Tip radius

The tip radii of Si_3N_4 tips coated with siloxane monolayers were determined by profiling them over atomically sharp features on the (305) face of $SrTiO_3$ annealed in O_2 at 1300°C [32]. Errors in the values of tip radii determined with this method were on the order of 10–20 nm (approx. 15%), as found from the fitting of multiple tip profiles taken at different locations on the surface of the $SrTiO_3$ sample.

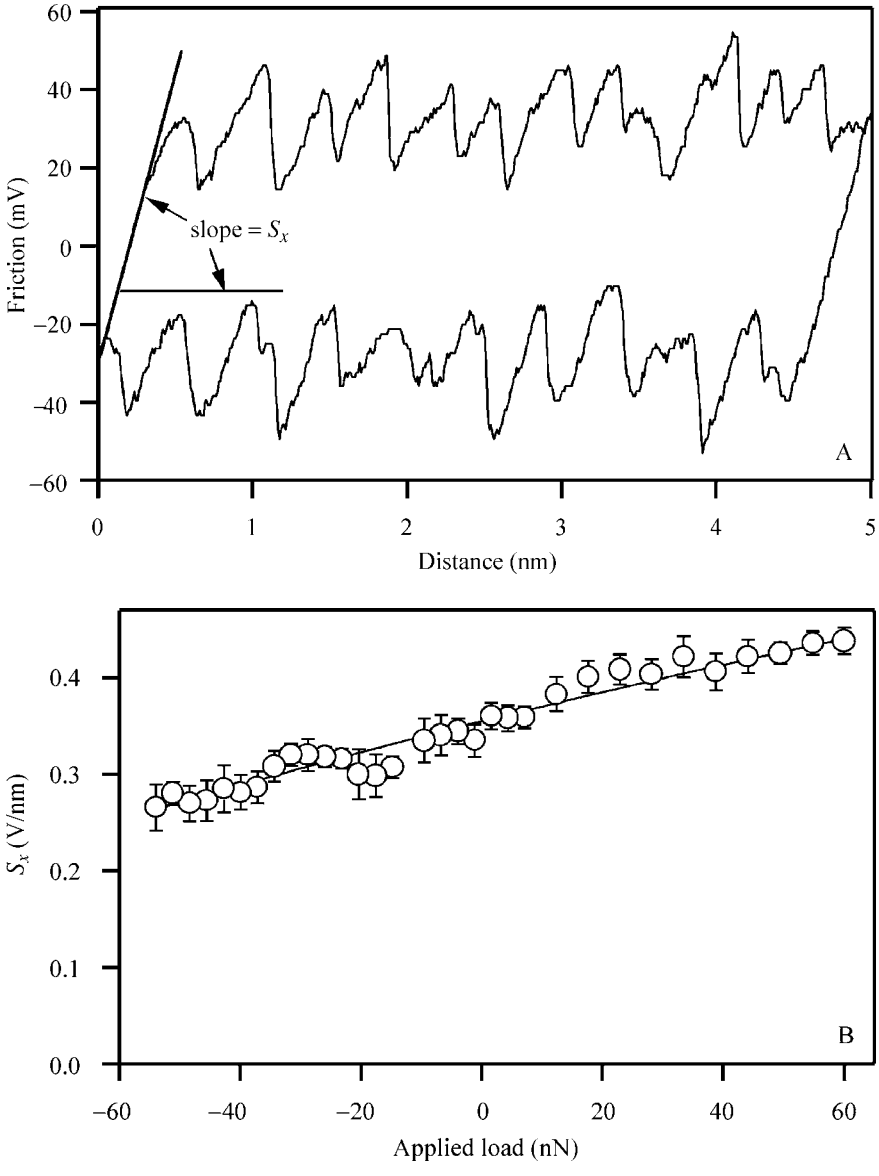

Figure 1. (A) Determination of the lateral sensitivity (S_x) of the photodiode detector from atomic stick–slip friction loops on mica. (B) Dependence of the lateral sensitivity determined in (A) on the external load applied to the tip.

3. RESULTS AND DISCUSSION

3.1. Friction between methyl terminated thiolate monolayers on Au

Friction forces between chemically modified tips and surfaces should be proportional to the number of interacting groups, or area of contact. At the same time,

friction force should also be proportional to the strength of the interaction between groups on the tip and sample, or interfacial shear strength. It is important to note that the contact mechanics models used to interpret the adhesion data in experiments with chemically-modified tips predicts a non-linear dependence for friction *versus* applied load when a single spherical tip contacts a planar surface.

Therefore, while characterization of the friction forces between organic surfaces of the SAMs in terms of the friction coefficients is acceptable when experiments are done under similar conditions (i.e. with the tips of comparable radii and similar material properties), a more fundamental quantity, such as interfacial shear strength, should be determined in friction experiments to de-couple the contact area effects and develop a fundamental understanding of the influence of the surface chemistry on the energy dissipation in friction. We first consider the possible reasons for the observed linear law in the friction (F) *versus* applied load (L) data reported in the literature for SAMs on Au systems studied in SPM setting [12, 14].

In most of our experiments with Au-modified tips and samples, the F–L curves were linear, in spite of the fact the adhesion data were consistent with a single asperity treatment within contact mechanics framework: a good correlation was observed between adhesion forces and surface free energy determined from contact angles [27]. In our opinion, the apparent linear form of the F–L curves stems from the averaging of multiple single-asperity contacts occurring when a friction loop is averaged over a path of several μm. The typical sizes of the Au grains were 50–200 nm for the Au films deposited at room temperature on Si substrates. The contributions from the multiple grains and grain boundaries, encountered in succession by the tip, are averaged in the calculation of the friction forces from the friction loops. The friction and topography images of the SAMs on Au were highly correlated. Thus, the substrate presents to a sliding probe a changing effective radius of curvature and a number of the grain boundaries — both causing variations in the friction forces. For small forces in organic media, the friction-force variation can be as high as 30–40% of the absolute average value. The quality and flatness of the Au film were also reported to affect the mean and the width of the distribution in adhesion force measurements [33].

Despite this averaging effect, the non-linear behavior, however, was detectable at small or tensile loads in the friction loop measurements for systems that exhibited large adhesion, such as hydrophobic SAMs in water. Large forces for relatively blunt tips turned substrate imperfections into secondary effects. Notably, F–L data acquired for CH_3-terminated SAMs in water (Fig. 2) show a prominent non-linear dependence on applied load. Assuming that the friction force can be expressed as a product of the interfacial shear strength, τ_0, and contact area, πa^2, the data in Fig. 2 are well-fitted to the contact area *versus* load dependence predicted by the Johnson–Kendall–Roberts (JKR) model:

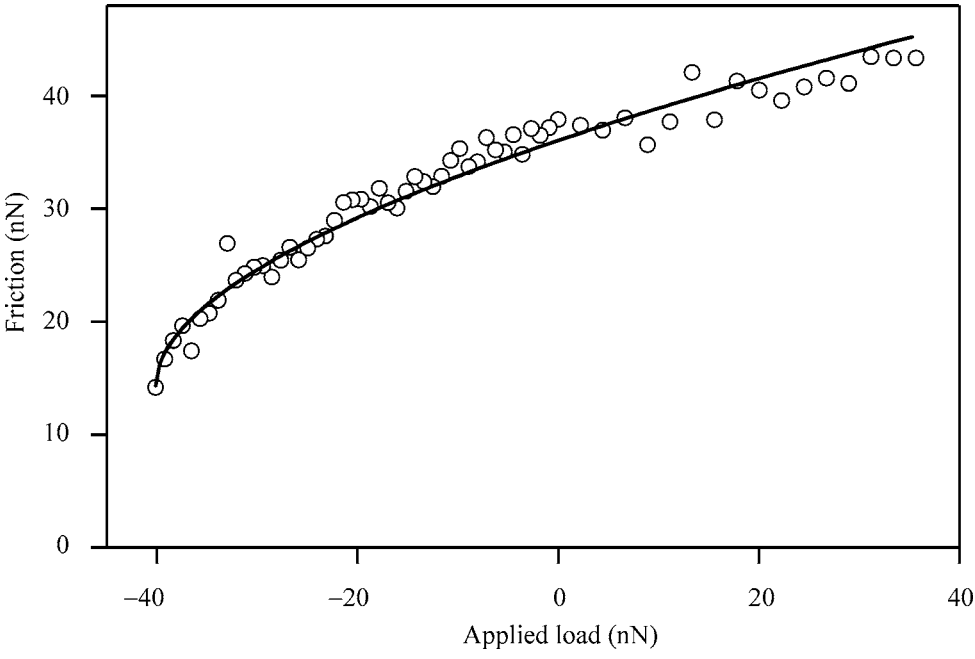

Figure 2. Friction force *versus* applied load curve (○) for a CH_3-terminated tip and sample in water. The concave shape of the curve is consistent with the non-linear dependence of the contact area on external load predicted by the JKR model, equation (1) (—). Absolute friction values are reported here without the adjustment for the contact stiffness in the detector calibration (they are about a factor of 1.5 higher than the actual values).

$$F = \tau_0 \pi a^2 = \pi \tau_0 \left(\frac{R}{K}\right)^{2/3} \left(L + 2L_0 + \sqrt{4L_0 L + (2L_0)^2}\right)^{2/3}$$
$$= F_0 \left(1 + \sqrt{1 + \frac{L}{L_0}}\right)^{4/3}, \qquad (1)$$

where

$$K = \frac{4}{3}\left(\frac{1-\nu_1^2}{E} + \frac{1-\nu_2^2}{E}\right)^{-1}$$

is the effective elastic constant of the system, L_0 is the pull-off force (in the JKR model $L_0 = 3\pi R\gamma$ for a symmetric contact, γ being the surface free energy) and $F_0 = \pi \tau_0 (L_0 \cdot R/K)^{2/3}$ is the friction force at the external load $L = -L_0$. These results demonstrate that on the basic level CFM experiments do probe friction arising from interactions within a single-asperity contact. Single-asperity contacts have also been reported for Si_3N_4 tips on bare [34] and siloxane-coated mica [35] and for monolayers of C_{60} on GeSe [36], for Si tips on NaCl [37], Pt-coated tips on mica [38, 39], and many other systems [2–7].

However, the substrate roughness was still apparent in this experiment in the large standard deviation of friction forces (10–20%) and a significant discrepancy in the pull-off forces determined in the stepwise dynamic (friction loops) and quasi-static (force curves) experiments — adhesion in the latter case being much greater (by almost a factor of 3). These problems led to an ambiguity in the value of the quantity $\tau_0/K^{2/3}$ found from the fit to the contact mechanics model: 10.3 $Pa^{1/3}$, if using apparent parameters (dynamic L_0) or 4.9 $Pa^{1/3}$, if using values obtained from the adhesion measurements. In addition, F–L data acquisition in a commercial instrument required stepwise increase in load and, thus, provisions for instrumental drift compensation had to be made. The need to use highly polar liquids, in which adhesion is extremely high, is also troublesome, because, as we have recently demonstrated [27], the deviations of the measured adhesion from the predictions of contact mechanics can become severe at these high forces.

The experiments with the thiol SAMs on Au pointed to the difficulties of obtaining quantitative information on interfacial shear strength between organic functional groups in this system and the need to move to (1) flat and smooth substrate/tip surfaces, (2) shorter sliding-loop paths and (3) higher quality friction measurements with simultaneous acquisition of the friction and load data. We addressed these issues by moving to a similar system of the SAMs on the surfaces of the silicon oxide (polished silicon substrates) and oxynitride (silicon nitride tips). Friction data were captured during a continuous sweep of the external load values by means of the AC technique originally described by Colchero *et al.* [28].

3.2. Friction between methyl terminated siloxane monolayers on oxide surfaces

Figure 2 shows typical friction force (F) *versus* external load (L) curves obtained with silicon nitride tips and silicon samples coated by octadecyltrichlorosilane (OTS) monolayers (CH_3-terminated). We used the same tip–sample pair to preserve geometrical constraints of the experimental setup and varied the surface energy by adjusting the properties of liquids. We have conducted a systematic study using a series of liquids with a varying degree of hydrogen-bonding ability (methanol/water mixtures) [27], so that the influence of the liquid induced adhesion variation could be understood and quantified.

As the amount of water in methanol gradually changes from 0 to 40 %, the pull-off force increases several-fold, and the friction force is detected at increasingly negative (tensile) loads. At the same time, the friction force measured at zero applied load also increases. However, if the contribution from the liquid displacement can be neglected, the liquid is excluded from the interface at which the energy dissipation due to friction takes place, and one expects friction forces at molecular scale (e.g. per SAMs unit cell or per functional group) to be independent of the surrounding medium under these conditions. Significantly, all the curves obtained under different conditions superimpose when plotted in the reduced coordinates (F/F_0

versus L/L_0) due to the exclusion of the liquid from the contact zone (Fig. 3). In this case, F_0 is the friction under zero applied load.

The non-linear shape of the F–L curve is characteristic of a single spherical asperity in contact with a flat substrate. To treat the friction data quantitatively, we have to adopt an appropriate contact mechanics model [40]. The correct choice is determined by the extent of surface deformation with respect to intermolecular surface forces. For hard contacting surfaces in AFM experimental geometry, the Derjaguin–Muller–Toporov (DMT) [41] regime should apply [40], although the results of the JKR model were found to apply in the case of blunt tips coated with soft metals [38, 39]. Since both silicon nitride and silicon are very stiff substrates (Young's moduli > 100 GPa), one expects that the DMT model should describe our results well. Indeed, the friction versus load curves can be fitted by the DMT-type relationship between the contact area and external force (Fig. 3):

$$F = \tau_0 \pi a^2 = \pi \tau_0 \left(\frac{R}{K}\right)^{2/3} (L + L_0)^{2/3} = F_0 \left(1 + \frac{L}{L_0}\right)^{2/3}. \tag{2}$$

The two models differ substantially in predicted contact area (the number of molecular contacts contributing to the overall interaction force), force of adhesion and surface profile. However, it was demonstrated [42] by numerical calculations based on the Lennard–Jones (L–J) potential that the DMT and JKR results represented the opposite ends of the spectrum of outcomes depending on the magnitude of the non-dimensional parameter μ (the so-called Tabor elasticity parameter):

$$\mu = \left(\frac{16}{9} \frac{RW^2}{K^2 z_0^3}\right)^{1/3}, \tag{3}$$

where z_0 is the equilibrium distance in the L–J potential. This parameter asserts the relative importance of the deformation under surface forces: for $\mu < 0.1$ the DMT model is valid, for $\mu > 5$ the JKR model applies. Using a z_0 value of 0.1 nm and reported [1] values of $K \approx 6.4$ GPa for thiol monolayers on Au, μ is in the range of 2.9–4.2 (depending on the adopted value of the adhesion force) for the data obtained for CH_3-terminated SAMs in water, clearly very close to the JKR regime. On the other hand, for the siloxane monolayers on silicon ($K \approx 10.3$ GPa) [1] in methanol/water mixtures we have $\mu = 0.5$–0.9 (depending on the composition), clearly closer to the DMT regime. There is also an uncertainty regarding whether elastic constants of the tip and substrate materials should be used rather than those of the organic monolayers, although the experimental numbers used above seem to agree with the latter. If the K values for substrate materials are used (64.5 GPa for Au and 120 GPa for Si/Si_3N_4), μ is reduced to 0.7–1.0 and 0.1–0.2 for the above two systems of thiols on Au and siloxanes on Si/Si_3N_4, respectively, pointing to a transition case for CH_3-terminated thiol SAMs in water and DMT regime for siloxane SAMs in water/methanol mixtures.

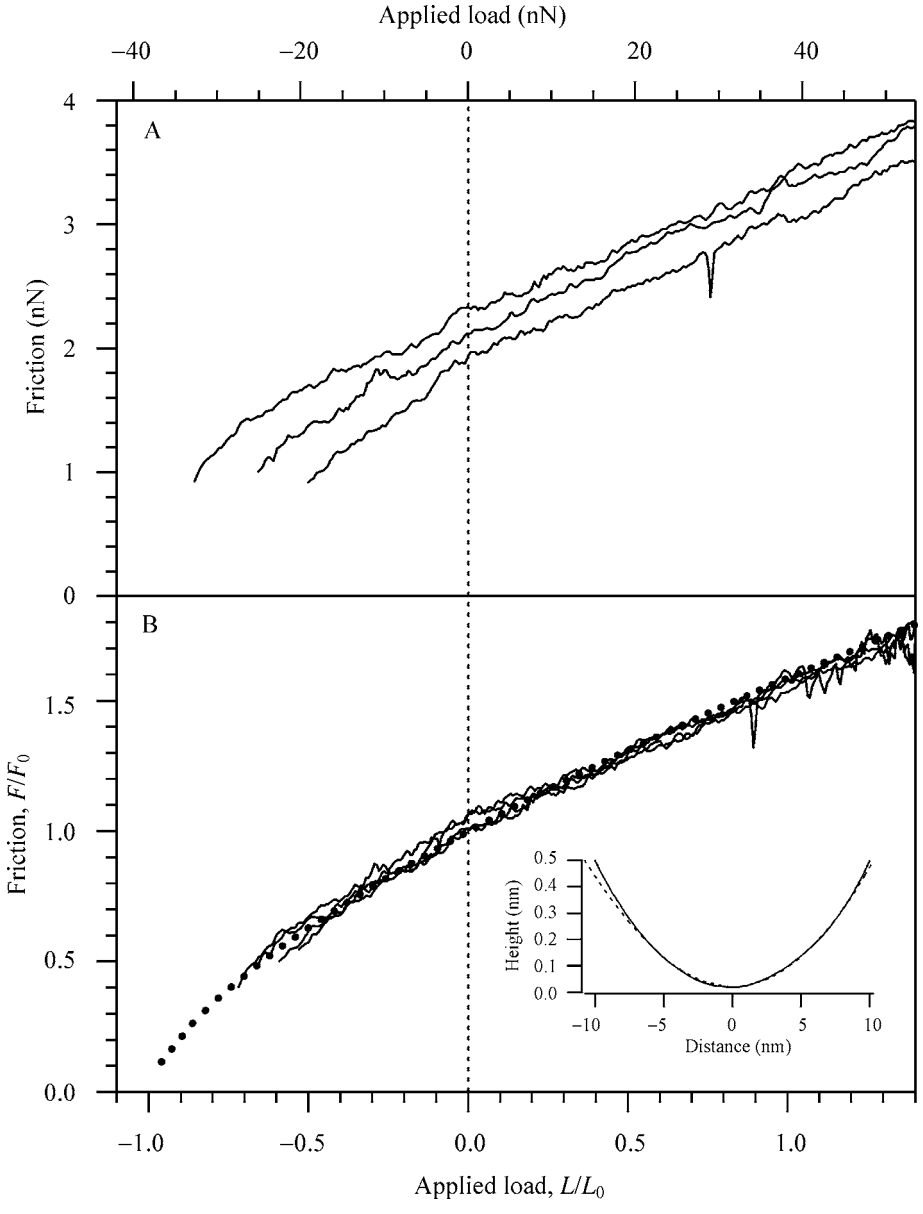

Figure 3. (A) Friction force *versus* applied load (top axis) curves for silicon nitride tips and silicon samples coated with OTS in methanol water mixtures at 60, 70 and 80 vol% of MeOH (from highest to lowest adhesion). (B) Friction force *versus* applied load (bottom axis) curves for silicon nitride tips and silicon samples coated with OTS in methanol water mixtures at 100, 90, 80, 70 and 60 vol% of MeOH (thin solid lines) plotted in reduced coordinates F/F_0 *versus* L/L_0, where F_0 is the friction at zero applied load and L_0 is absolute value of the external load at zero friction. Each line is an average of approximately 100 measurements. Theoretical predictions of the DMT model are also shown (thick dotted line). Inset: profile of the last 0.5 nm of the tip apex used in one of the experiments, which was determined by imaging sharp features on $SrTiO_3$ (305) surface. Solid and dashed lines correspond to two mutually perpendicular profiles.

For the sphere-on-plane contact mechanics problem, self-consistent calculations based on a specific potential (such as L–J) can be avoided by using the analytical solution produced by Maugis [43]. The Maugis model invoked the Dugdale approximation that the stress due to molecular attraction had a constant value σ_0 (theoretical stress) until a separation $h_0 = W/\sigma_0$ was reached at the contact zone radius, whereupon it fell to zero. The difficulty with the Maugis–Dugdale (MD) theory is that it does not easily lend itself to fitting the experimental data. Although the JKR model clearly failed in the case of the siloxane SAM system, we found no substantial improvements in the goodness of the fit when performing non-linear fitting of our data to MD equations with different small values of μ (<0.2). Therefore, we will use the limiting case of DMT contact mechanics in the analysis of numerical values of the fitted parameters.

From this kind of analysis, one can extract, in principle, the value of the interfacial shear strength. The knowledge of the tip radius, R, and effective elastic constant, K, of the composite Si_3N_4/OTS/OTS/Si system is needed, however. The tip radius can be determined from the imaging of sharp features such as those on the (305) surface of annealed $SrTiO_3$ [32]. However, the estimates of the elastic constants are less certain and, therefore, the data not requiring further assumptions in the interpretation are presented in the form of $\tau_0/K^{2/3}$, which is sufficient for our purposes here, since the effective K remains constant for a fixed tip–sample combination when the liquid is exchanged.

Data on the interfacial shear strength deduced from the fits to equation (2) for OTS surfaces in the methanol/water mixtures are compiled in Table 1 and presented in Fig. 4 as a function of the measured adhesion force. Despite almost an order of magnitude change in the adhesion force, the frictional dissipative interactions are not affected. Thus, we may conclude that liquid (1) appears to be excluded from the contact zone and (2) has practically no effect on the interactions within that zone, i.e. the main effect of the liquid medium is to change the contact area between the tip and substrate surfaces. The change in adhesion interactions caused by the change in the interfacial chemistry, on the other hand, has been shown to affect frictional forces significantly [12, 14]. The fact that displacement of the liquid from the adjacent areas by the sliding tip does not contribute detectably to energy dissipation in our system does not necessarily extend to friction under liquids in all other systems. An apolar interface provided by the CH_3-terminated SAM interacts with the liquid via dispersion forces and is not capable of forming strong directional bonds with the molecules of the liquid. However, the contribution of displacement of the liquid may become significant in the case of associating liquids forming a structured layer at the solid interface of high surface energy, for example, via hydrogen bonding. Further work on the single asperity friction in the strongly interacting systems will be needed to address this issue.

Table 1.
Surface free energy (γ) from contact angle measurements, adhesion (L_0), tip radius (R) and interfacial shear strength ($\tau_0/K^{2/3}$) values between methyl-terminated SAMs under polar liquid media

	Interface									
	Au/SAM – SAM/Au	Silicon nitride (tip)/SAM – SAM/Silicon (sample)								
Medium	$CH_3OH:H_2O$	$CH_3OH:H_2O$	$CH_3OH:H_2O$	$CH_3OH:H_2O$	$CH_3OH:H_2O$	$CH_3OH:H_2O$	$CH_3OH:H_2O$	$CH_3OH:H_2O$	$CH_3OH:H_2O$	$CH_3OH:H_2O$
Ratio	0:100	100:0	90:10	80:20	70:30	60:40	90:10	80:20	70:30	60:40
γ (mJ/m^2)	52	2.8	5.5	7.5	8.8	10.4	5.5	7.5	8.8	10.4
L_0 (nN)	40	8.3 ± 0.9	12.1 ± 1.7	20.3 ± 2.3	14.2 ± 1.7	19.2 ± 2.9	29.5 ± 3.7	32.7 ± 3.3	39.8 ± 4.5	39.3 ± 4.0
R (nm)	120	74 ± 10	74 ± 10	74 ± 10	74 ± 10	74 ± 10	147 ± 20	147 ± 20	147 ± 20	147 ± 20
$\tau_0/K^{2/3}$ ($Pa^{1/3}$)	10.3	2.13 ± 0.32	1.99 ± 0.30	2.20 ± 0.32	2.13 ± 0.32	2.70 ± 0.42	2.00 ± 0.29	2.02 ± 0.29	2.06 ± 0.29	2.12 ± 0.04

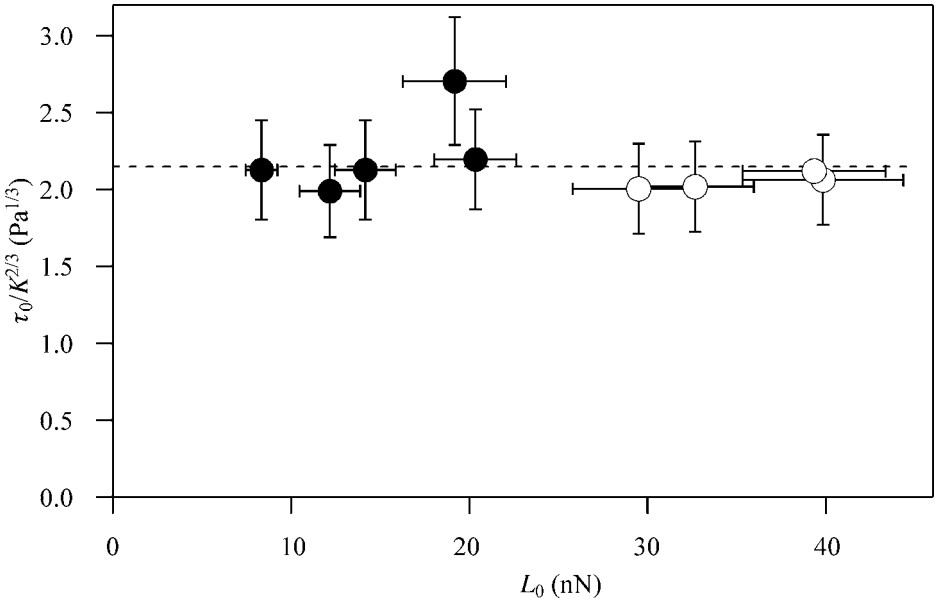

Figure 4. Interfacial shear strength, τ_0, normalized by the elastic constant, $K^{2/3}$, *versus* the force of adhesion measured simultaneously from the curves of the type shown in Fig. 3. Error bars represent standard deviations from the mean values found in the analysis of approximately 100 single curves. Closed and open symbols represent two different experiments.

3.3. Comparison of the interfacial shear strength of the SAMs under liquids and interfacial shear strengths in similar systems

The average value of $\tau_0/K^{2/3} = 2.15 \pm 0.22$ Pa$^{1/3}$ for OTS monolayers is much lower than the values of 158 Pa$^{1/3}$ found between carbon films (amorphous carbon and diamond) and amorphous carbon-coated Si tips and approaches 1.2 Pa$^{1/3}$ observed for the graphite–amorphous carbon interface [5]. This finding suggests that siloxane SAMs can be much more effective in reducing wearless friction than various vacuum-deposited carbon layers. Our $\tau_0/K^{2/3}$ values compare favorably with an independent interfacial force microscopy (IFM) study [1] of friction between a glass tip and the CH_3-terminated thiol SAM on Au, where it was found $\tau_0 = 13.7 \pm 1.5$ MPa or $\tau_0/K^{2/3} = 2.8 \pm 0.3$ Pa$^{1/3}$ (with $K = 11$ GPa for the Au/SAM-glass case). If we use K values for SAMs experimentally determined in Ref. [1] with our data, we can calculate interfacial shear strength between CH_3-terminated surfaces as 10.2 ± 1.0 MPa for the siloxane SAM on Si ($K = 10.3$ GPa) and 16.7–35.5 MPa for the thiol SAM on Au ($K = 6.4$ GPa). We believe that the discrepancy is mostly due to the limited accuracy in the adopted calibration procedures and probe characterization, although a more direct comparison may be necessary to confirm this. In general, these values for organic surfaces of closely-packed crystalline SAMs are substantially lower than the interfacial shear strength typically observed between inorganic interfaces [2–6, 17].

The friction experiments conducted with a scanning force microscope suffer from the inability to measure tip–sample relative displacement independently, unlike in the IFM setup [1]. Consequently, the elastic constants cannot be evaluated from these experiments and derivation of absolute values of τ_0 requires knowledge of the reliable values of elastic constants. The effective Young's modulus for a monolayer film on a stiff substrate is difficult to measure or to calculate, thus, scarce results for K values, such as those obtained from IFM studies, are very important. IFM-based Young's modulus of 8 GPa and 13 GPa for thiol and siloxane SAMs are very close to the range of 5–10 GPa expected for high-density polyethylene. Therefore, elastic properties of the contact are dominated by the soft ultrathin film, rather than by the stiff substrate.

This somewhat unexpected observation is consistent, however, with the theoretical model of the Hertzian (i.e. DMT-like) deformation of the thin film on an elastic substrate by an elastic sphere [44]. The deviation of the contact area from that expected for the film bulk material begins when the expected radius of the contact area, a, exceeds the film thickness, t, i.e. $t/a < 1$. However, for large relative magnitudes of Young's moduli as in our systems, the deviation is approx. 10% for $t/a = 0.1$, but reaches approx. 30% for $t/a = 0.01$. With the above values of τ_0, the ratio t/a changes from 0.5 to 0.2 for the data in Fig. 3 and from 0.3 to 0.2 for the data in Fig. 2; hence, contact-area changes in our experiments are dominated by the elastic properties of the SAMs. Therefore, the use of the low K is consistent with the observed magnitude of the friction force and the data are expected to be adequately described with a single K value and only a slight underestimation of τ_0 (as determined from the experimental $\tau_0/K^{2/3}$ ratio). Since friction measurements between surfaces modified by thin films (including SAMs) are increasingly more common, additional experimental and theoretical (or numerical modeling) work is highly desirable to describe the effective elastic constants in these systems.

It is also instructive to compare our CFM results on interfacial shear strength values to recently reported macroscopic measurements with a sapphire ball-on-the-surface apparatus [45]. Since polished Si substrates were used in that work, a sphere-on-flat contact appeared to be valid in that case, because, similarly to our experiments, the friction data could be fitted to contact area predictions from the contact mechanics theories. The surface modification of the Si with the OTS monolayer and diamond-like carbon (DLC) confirmed a significant reduction in friction (more than an order of magnitude), with the DMT-like fits yielding $\tau_0/K^{2/3}$ of 0.073 and 0.50 $\mathrm{Pa}^{1/3}$ for OTS and DLC-modified Si, correspondingly. The interfacial shear strength (in the form of $\tau_0/K^{2/3}$ values) found from these macroscopic tests, however, are almost two orders of magnitude lower than in the nanometer-scale single-asperity experiments described here and carried out by others [1, 5]. The observation of the much lower $\tau_0/K^{2/3}$ values is consistent with a lower true area of contact and, thus, with a multi-asperity contact, in spite of the microscopic flatness of the Si substrate and in spite of the fact that, formally, the overall deformation could be described by an apparent sphere-on-flat single contact.

4. CONCLUSIONS

Measurements of the friction forces between chemically-modified tips and samples under liquids strongly indicate that these experiments achieve a single-asperity contact. Changes in the contact area can be quantitatively described by the appropriate contact mechanics models, and interfacial shear strengths between organic functional groups can then be determined. The interfacial shear strength for CH_3-terminated surfaces was independent of the overall adhesion force (surface free energy) when the adhesion level changed due to the variations in the liquid. The CFM results in liquids are in good agreement with the interfacial shear strength values determined for these systems in the gas environments using an interfacial force microscope. Therefore, changes in adhesion due to differences in the solid–liquid interfacial free energy, as measured by the CFM experiments, do not affect energy dissipation at the solid–solid interface, which apparently dominates friction forces in these systems. This point is extremely important for drawing correlations between adhesion and frictional forces in liquids for the chemically modified surfaces. Friction measurements using SAM samples prepared on polycrystalline gold surfaces suffer from imperfection of the substrate surface, which can prevent the experiments from revealing the single asperity nature of the probe-sample contact. Analysis of our results and available literature data also demonstrates that chemically attached organic monolayers are much more effective in reducing interfacial shear strength than various carbon (amorphous carbon, DLC and diamond) coatings.

Acknowledgements

C. M. L. acknowledges support for this work from the Air Force Office of Scientific Research.

REFERENCES

1. A. R. Burns, J. E. Houston, R. W. Carpick and T. A. Michalske, *Langmuir* **15**, 2922 (1999).
2. M. Enachescu, R. J. A. Vandenoetelaar, R. W. Carpick, D. F. Ogletree, C. F. J. Flipse and M. Salmeron, *Phys. Rev. Lett.* **81**, 1877 (1998).
3. M. A. Lantz, S. J. Oshea and M. E. Welland, *Phys. Rev. B* **56**, 15345 (1997).
4. R. W. Carpick and M. Salmeron, *Chem. Rev.* **97**, 1163 (1997).
5. U. D. Schwarz, O. Zworner, P. Koster and R. Wiesendanger, *Phys. Rev. B* **56**, 6987 (1997).
6. U. D. Schwarz, O. Zworner, P. Koster and P. Wiesendanger, *Phys. Rev. B* **56**, 6997 (1997).
7. M. A. Lantz, S. J. Oshea, A. C. F. Hoole and M. E. Welland, *Appl. Phys. Lett.* **70**, 970 (1997).
8. D. F. Ogletree, R. W. Carpick and M. Salmeron, *Rev. Sci. Instrum.* **67**, 3298 (1996).
9. U. D. Schwarz, P. Koster and R. Wiesendanger, *Rev. Sci. Instrum.* **67**, 2560 (1996).
10. J. L. Hutter and J. Bechhoefer, *Rev. Sci. Instrum.* **64**, 1868 (1993).
11. J. P. Cleveland, S. Manne, D. Bocek and P. K. Hansma, *Rev. Sci. Instrum.* **64**, 403 (1993).
12. A. Noy, D. V. Vezenov and C. M. Lieber, *Annu. Rev. Mater. Sci.* **27**, 381 (1997).

13. B. Bhushan, in: *IEEE Proceedings of the Ninth Annual International Workshop on Micro Electro Mechanical Systems. An Investigation of Micro Structures, Sensors, Actuators, Machines and Systems. Nanotribology and Nanomechanics of MEMS Devices*, p. 91 (1996).
14. V. V. Tsukruk, *Adv. Mater.* **13**, 95 (2001).
15. C. D. Frisbie, L. F. Rozsnyai, A. Noy, M. S. Wrighton and C. M. Lieber, *Science* **265**, 2071 (1994).
16. A. Schumacher, N. Kruse, R. Prins, E. Meyer, R. Lijthi, L. Howald, H.-J. Güntherodt and L. Scandella, *J. Vac. Sci. Technol. B* **14**, 1264 (1996).
17. M. A. Lantz, S. J. Oshea, M. E. Welland and K. L. Johnson, *Phys. Rev. B* **55**, 10776 (1997).
18. A. Noy, C. D. Frisbie, L. F. Rosznyai, M. S. Wrighton and C. M. Lieber, *J. Am. Chem. Soc.* **117**, 7943 (1995).
19. J.-B. D. Green, M. T. McDermott, M. D. Porter and L. M. Siperko, *J. Phys. Chem.* **99**, 10960 (1995).
20. D. V. Vezenov, A. Noy, L. F. Rozsnyai and C. M. Lieber, *J. Am. Chem. Soc.* **119**, 2006 (1997).
21. H. Yoshizawa and J. Israelachvili, *Thin Solid Films* **246**, 1 (1994).
22. J. Israelachvili, *Acc. Chem. Res.* **20**, 415 (1987).
23. J. Israelachvili, *J. Vac. Sci. Technol. A* **10**, 2961 (1992).
24. Y. L. Chen, C. A. Helm and J. N. Israelachvili, *J. Phys. Chem.* **95**, 10736 (1991).
25. H. Yoshizawa, Y. L. Chen and J. Israelachvili, *J. Phys. Chem.* **97**, 4128 (1993).
26. A. Lio, D. H. Charych and M. Salmeron, *J. Phys. Chem. B* **101**, 3800 (1997).
27. D. V. Vezenov, A. V. Zhuk, G. M. Whitesides and C. M. Lieber, *J. Am. Chem. Soc.* **124**, 10578 (2002).
28. J. Colchero, M. Luna and A. M. Baro, *Appl. Phys. Lett.* **68**, 2896 (1996).
29. Y. Liu, T. Wu and D. F. Evans, *Langmuir* **10**, 2241 (1994).
30. R. W. Carpick, D. F. Ogletree and M. Salmeron, *Appl. Phys. Lett.* **70**, 1548 (1997).
31. J. L. Hazel and V. V. Tsukruk, *Thin Solid Films* **339**, 249 (1999).
32. S. S. Sheiko, M. Moller, E. M. C. M. Reuvekamp and H. W. Zandbergen, *Phys. Rev. B* **48**, 5675 (1993).
33. R. McKendry, M.-E. Theoclitou, C. Abell and T. Rayment, *Langmuir* **14**, 2846 (1998).
34. C. Putman and R. Kaneko, *Thin Solid Films* **273**, 1 (1996).
35. X. Xiao, J. Hu, D. H. Charych and M. Salmeron, *Langmuir* **12**, 235 (1996).
36. U. D. Schwarz, W. Allers, G. Gensterblum and R. Wiesendanger, *Phys. Rev. B* **52**, 14976 (1995).
37. E. Meyer, R. Luthi, L. Howald, M. Bammerlin, M. Guggisberg and H.-J. Güntherodt, *J. Vac. Sci. Technol. B* **14**, 1285 (1996).
38. R. W. Carpick, N. Agrait, D. F. Ogletree and M. Salmeron, *J. Vac. Sci. Technol. B* **14**, 1289 (1996).
39. R. W. Carpick, N. Agrait, D. F. Ogletree and M. Salmeron, *Langmuir* **12**, 3334 (1996).
40. K. L. Johnson, *Proc. Royal Soc. London A* **453**, 163 (1997).
41. B. V. Derjaguin, V. M. Muller and Yu. P. Toporov, *J. Colloid Interface Sci.* **53**, 314 (1975).
42. V. M. Muller, V. S. Yushchenko and B. V. Derjaguin, *J. Colloid Interface Sci.* **77**, 91 (1980).
43. D. Maugis, *J. Colloid Interface Sci.* **150**, 243 (1992).
44. M. G. D. El-Sherbiney and J. Halling, *Wear* **40**, 325 (1976).
45. H. Liu, S. I.-U. Ahmed and M. Scherge, *Thin Solid Films* **381**, 135 (2001).